

MULTI-LEVEL KONDO REGIMES IN A QUANTUM DOT

S. DE FRANCESCHI¹, W. G. VAN DER WIEL¹, T. FUJISAWA², J. M. ELZERMAN¹,
W. IZUMIDA^{2,3}, S. TARUCHA^{2,3}, L. P. KOUWENHOVEN¹

¹*Department of Applied Physics, DIMES, and ERATO Mesoscopic Correlation Project, Delft University of Technology, PO Box 5046, 2600 GA Delft, The Netherlands*

²*NTT Basic Research Laboratories, Atsugi-shi, Kanagawa 243-0198, Japan*

³*ERATO Mesoscopic Correlation Project, University of Tokyo, Bunkyo-ku, Tokyo 113-0033, Japan*

In a recent work (van der Wiel *et al.*, Science **289**, 2105 (2000)) we studied the transport properties of a semiconductor quantum dot connected to one-dimensional leads. A strong Kondo effect was found under proper conditions, which followed the essential expectations from the Anderson impurity model, including the achievement of ideal conductance (i.e. $G = 2e^2/h$) at low temperatures (unitary limit). Here we push our analysis to a deeper level. We present a first attempt to fit the linear-response characteristics at different temperatures using the numerical-renormalisation-group technique. Although we obtain reasonable agreement for the lowest temperature, significant deviations appear at higher temperatures which may be due to the multi-level structure of the dot. Further signatures of multi-level physics emerge in the dependence of the tunnel conductance on a magnetic field perpendicular to the dot plane. In the range between 0 and 2 T, we find a rich variety of Kondo regimes that cannot be explained in terms of a single-level model.

The Kondo effect arises from the many-body interaction between conduction electrons and a localised spin, usually provided by a magnetic impurity embedded in a non-magnetic metal¹. Recent developments in the field of nanotechnology have opened new perspectives for a deeper study of Kondo-related phenomena². In 1988 it was pointed out that quantum dots could behave as artificial magnetic impurities and exhibit the Kondo effect³. Unlike the case of a metal containing magnetic impurities, the Kondo effect is expected to enhance the conductance, G , of a quantum dot device. This follows from the fact that electrons have to go through the quantum dot in order to contribute to transport. In this case the Kondo resonance facilitates mixing between the states belonging to the two opposite leads, resulting in an increased G . For the case of equal-transmissivity barriers, G can reach $2e^2/h$ (unitary limit) at temperatures much smaller than the Kondo temperature, T_K .

The first observations of the Kondo effect in a quantum-dot device were reported in 1998, however without reaching the unitary limit⁴. The results of these experiments followed reasonably well the expectations from the Anderson impurity model⁵. In this model the quantum dot has only one spin-degenerate level with energy ϵ_0 and line-width $\Gamma = \Gamma_l + \Gamma_r$, where Γ_l and Γ_r are the tunnel rates associated with the two tunnel barriers. The on-site Coulomb repulsion allows only one electron to sit on the dot so that the local spin, S , is equal to 1/2. Following experiments^{6,7,8} have brought up more data to be compared with theoretical predictions. Here we intend to address this issue and present some experimental results for which we haven't found a satisfactory explanation yet.

All of the measurements reported in this article were performed on the same quantum dot studied in Ref. 8. The device was fabricated from an AlGaAs/GaAs heterostructure grown by molecular beam epitaxy on semi-insulating GaAs. A modulation-doped AlGaAs/GaAs heterojunction was used to create a two-dimensional electron gas (2DEG) with a density of $2.6 \times 10^{15} \text{ m}^{-2}$, 100 nm below the surface. The quantum dot was formed inside a one-dimensional wire defined in the 2DEG by dry etching (top-left inset to Fig. 1A). Quantum confinement was established by means of two transverse gates. We indicate by V_{gl} and V_{gr} the corresponding voltages. All measurements were performed in a dilution refrigerator with a base temperature

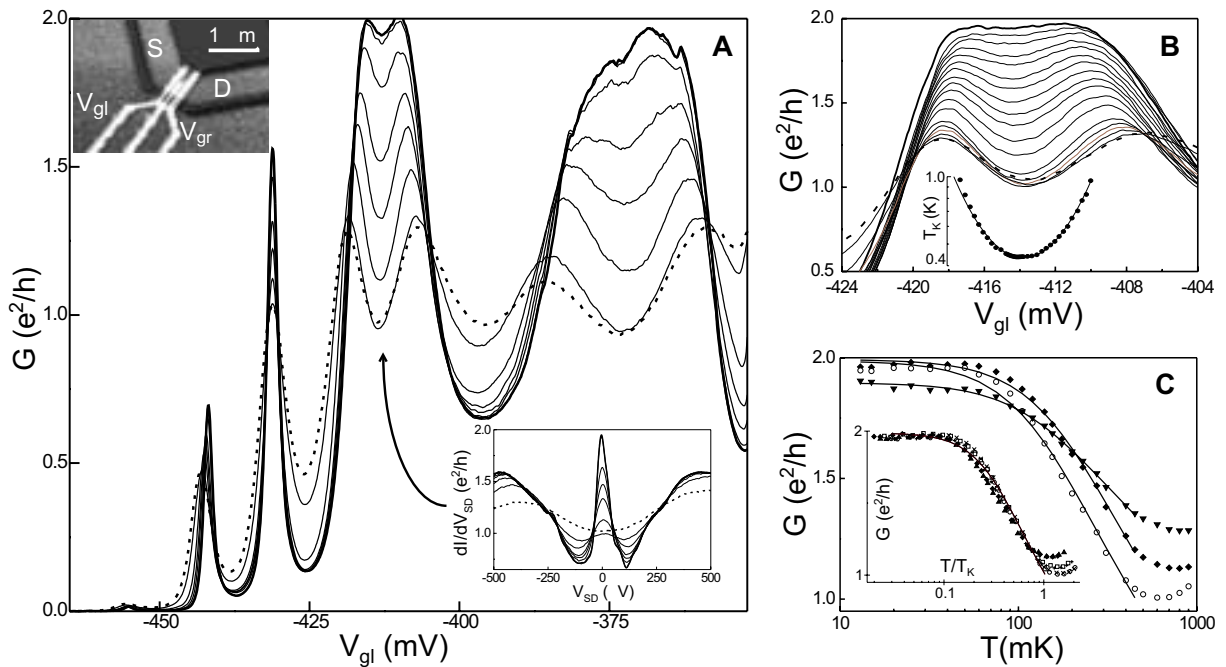


Figure 1: (A) Coulomb oscillations in G versus V_{gl} at $B = 0.4$ T for different temperatures. $T = 15$ mK (thick solid trace) up to 800 mK (thick dashed trace). V_{gr} is fixed at -448 mV. Top-left inset: atomic force microscope image of the device. Bottom-right inset: differential conductance, dI/dV_{SD} , versus dc bias voltage, V_{SD} , for $T = 15$ mK (thick solid trace) up to 900 mK (thick dashed trace), at $V_{gl} = -413$ mV and $B = 0.4$ T. The Kondo resonance manifests itself as a peak in dI/dV_{SD} at zero bias. (B) $G(V_{gl})$ around the Kondo plateau in the case of optimised symmetric tunnel barriers. T ranges between 15 mK (thick solid trace) up to 800 mK (thick dashed trace). Inset: Kondo temperature, T_K , at the Kondo plateau as obtained from many fits as in (C); the solid line is a parabolic fit of $\text{Log}(T_K)$ versus V_{gl} . (C) $G(T)$ at fixed gate voltage for $V_{gl} = -411$ (solid diamonds), -414 (open circles) and -418 (solid triangles) mV. The solid curves are fits as explained in the text. Inset: G versus normalised temperature, T/T_K , for six different gate voltages. All traces are fitted to a single curve (solid line).

$T = 15$ mK, using a standard lock-in technique with an ac voltage excitation between source and drain contacts of $3 \mu\text{V}$.

Figure 1 contains some essential results from Ref. 8. In Fig. 1A the conductance, G , is plotted as a function of gate voltage V_{gl} for different temperatures. All traces were taken in a magnetic field $B = 0.4$ T perpendicular to the 2DEG. At base temperature, conductance in the valleys around $V_{gl} = -413$ mV and -372 mV reaches the value of $2e^2/h$. In fact, the valleys tend to disappear. When the temperature is increased, two separate Coulomb peaks develop with growing peak spacing. The adjacent Coulomb valleys show an opposite T -dependence. This even-odd asymmetry suggests a pairwise filling of the dot levels, i.e. an unpaired spin in a valley with $N=\text{odd}$, where we observe the Kondo effect, and a spin singlet for $N=\text{even}$. In the right inset to Fig. 1A we show the differential conductance, dI/dV_{SD} , versus source-drain bias, V_{SD} , for different T in the middle of the Kondo plateau at $V_{gl} = -413$ mV. The pronounced peak around $V_{SD} = 0$ reflects the Kondo resonance at the Fermi energy. We note that since the Zeeman splitting for $B = 0.4$ T is several times smaller than $k_B T_K$ the Kondo resonance is not split by the magnetic field. The peak height (i.e. the linear conductance) has a logarithmic T -dependence with a saturation at $2e^2/h$ for low T denoting the achievement of the unitary limit. The unitary limit implies that the transmission probability through the quantum dot is equal to one. Although U is an order of magnitude larger than $k_B T_K$, the Kondo effect completely determines electron tunneling at low energies (i.e. $T \ll T_K$ and $eV_{SD} \ll k_B T_K$).

These measurements were taken after optimizing the two barrier gate voltages, V_{gl} and V_{gr} , in order to obtain nearly equal tunnel barriers. However, sweeping V_{gl} , as in Fig. 1A,

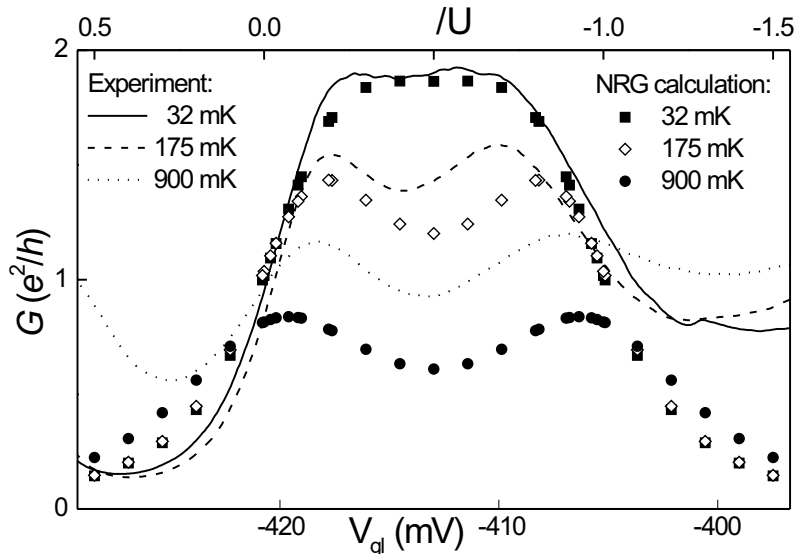


Figure 2: Comparison between linear-response measurements and numerical results obtained with the numerical renormalisation-group (NRG) method. The bottom scale (V_{gl}) is associated with the measured conductance traces (lines). The top scale (ϵ_0/U) refers to the numerical results (dots).

changes the left barrier much more effectively than the right one and hence the barriers cannot be symmetric over the whole V_{gl} -range. For a quantitative comparison to theory, we chose V_{gr} such that, upon sweeping V_{gl} , we could obtain a flat plateau close to $2e^2/h$ (Fig. 1B). The two discernable Coulomb oscillations at the highest temperatures have completely merged together at low T . In Fig. 1C we fit G versus T for different gate voltages to the empirical function $G(T) = G_0 [T_K'^2 / (T^2 + T_K'^2)]^s$. This function is an analytical approximation to numerical renormalisation-group (NRG) results for the Anderson impurity model⁹. $T_K' = T_K / \sqrt{2^{1/s} - 1}$ and s is a fit parameter that should be close to 0.2 for a spin-1/2 impurity. Indeed we find $s = 0.29$ and good agreement between experimental data and theoretical curves. The inset to Fig. 1B shows T_K versus V_{gl} as obtained from many fits as in Fig. 1C. $\text{Log}(T_K)$ follows a quadratic dependence on V_{gl} (i.e., ϵ_0) with a minimum in the middle of the conductance plateau. From the parabolic fit we estimate $U = 0.5$ meV and $\Gamma = 0.23$ meV (see Ref. 8 for more details). All over the plateau, G is a universal function of the normalised temperature, T/T_K , regardless of the other energy scales, U , ϵ_0 and Γ (see inset to Fig. 1C).

The results presented so far follow quite well some essential expectations from the Anderson impurity model. These expectations include the unitary limit, the parabolic dependence of $\text{Log}(T_K)$ on V_{gl} , and the scaling behavior in Fig. 1C. As we shall see below the Anderson model has also important limitations.

In Fig. 2 we compare some $G(V_{gl})$ curves measured at different temperatures with NRG results. The NRG data are plotted as a function of ϵ_0/U (top scale). All of the calculated traces are obtained using only one fitting parameter defined as $\Delta/\pi U$, where $\Delta = \Gamma/2$ (a detailed description of the numerical technique is given in Ref. 10). For a direct comparison with the experimental curves we used the linear relation $\epsilon_0 = \alpha V_{gl} + c$, where $\alpha = 45$ $\mu\text{eV}/\text{mV}$ and c is an adjustable constant. The best agreement is obtained for $\Delta/\pi U = 0.05$ and $U = 0.7$ meV, which is somewhat larger than the value reported above. With $\Gamma = 0.23$ meV we obtain $\Delta/\pi U = 0.052$ consistent with the value employed in the calculations. At the lowest temperature

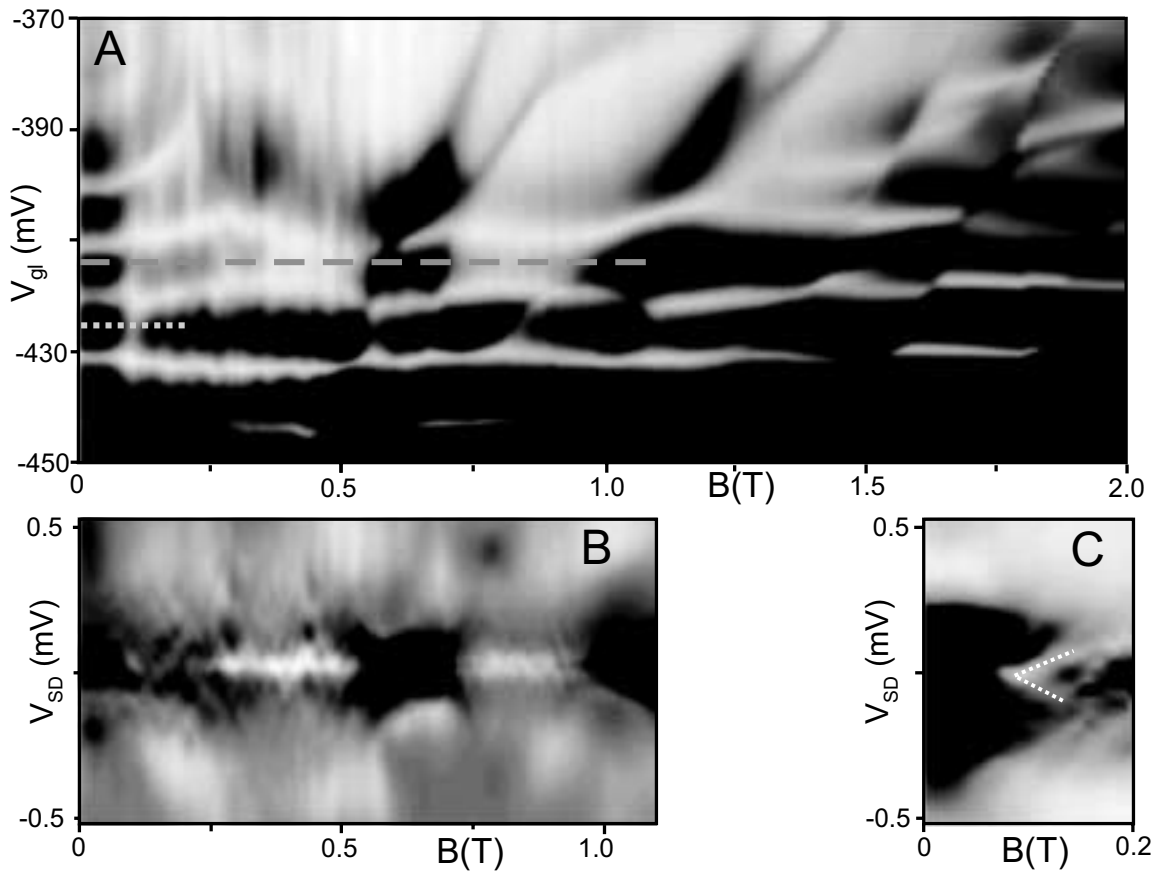


Figure 3: (A) Linear conductance G as a function of magnetic field, B , and gate voltage, V_{gl} . (B) Differential conductance, dI/dV_{SD} , versus B and dc bias voltage, V_{SD} at the dashed line in (A). (C) $dI/dV_{SD}(B, V_{SD})$ at the dotted line in (A). In (A), (B), and (C) light grey corresponds to values of order e^2/h .

(32 mK) NRG results reproduce fairly well the experimental conductance in the Kondo plateau and in the adjacent mixed-valence regimes. Away from this region, however, the numerical data deviate significantly from the experimental trace. This discrepancy is probably due to the V_{gl} -dependence of the tunnel rates Γ_r , and especially Γ_l . This effect is not taken into account in our NRG model which assumes $\Gamma_l = \Gamma_r = \Gamma/2 = \text{constant}$ over the shown energy range.

The agreement between theory and experiment is rather poor at higher temperatures. In the Kondo valley the NRG conductance decreases with T more rapidly than in the experiment. We seriously doubt that such a deviation could be cured by an improved control over the parameters involved in our calculation. Instead we suspect that the enhanced conductance denotes the contribution of excited states with energies close to the ground-state level. Increasing temperature may activate tunneling processes via these states.

We now discuss the effect of a magnetic field applied perpendicularly to the 2DEG plane. This will bring further evidence that multi-level effects can be very important.

In Fig. 3A G is plotted on grey scale as a function of V_{gl} and B . Dark regions have low conductance and correspond to the Coulomb blockade regimes. Light grey corresponds to $G \sim e^2/h$. The number of confined electrons increases with V_{gl} , but it is essentially independent of B . In spite of this fact, by varying B at a constant V_{gl} the linear conductance undergoes pronounced variations on a B -scale of 0.1 T. This unusual behaviour is most apparent in the middle part of the V_{gl} -range shown. In this regime the tunnel rates of the barriers are enhanced, however, without implying a substantial suppression of the Coulomb blockade effect. This is the condition for observing the strongest Kondo behaviour. We then ascribe the observed conductance

modulations to variations in the Kondo temperature. To prove this we have measured dI/dV_{SD} versus V_{SD} along the dashed and the dotted lines in Fig. 3A. The results are shown in Figs. 3B and 3C, respectively.

The dashed line is at $V_{gl} = -413$ mV. Along this line N is constant and presumably odd as argued in our analysis of Fig. 1. We find a strong Kondo resonance between 0.3 and 0.5 T (which explains our choice of $B = 0.4$ T for the measurements in Fig. 1); another Kondo resonance is found between 0.75 and 0.9 T. Here the field is strong enough to induce an appreciable splitting of the Kondo resonance, which is slightly visible in Fig. 3B.

Along the dotted line N is presumably even. We find a zero-bias resonance at $B = 0.1$ T. The resonance splits for $B > 0.1$ T as emphasised by the dotted lines in Fig. 3C. These features resemble those of the singlet-triplet Kondo effect observed in an integer-spin vertical quantum dot⁶ (an extensive discussion of this effect can be found in Ref. 11). According to this interpretation, we believe that the ground state is a triplet for $B < 0.1$ T and becomes a singlet for $B > 0.1$ T. An enhanced Kondo effect takes place at the degeneracy point. The Kondo resonance splits at higher B following the singlet-triplet splitting (as in Ref. 6, the splitting of the Kondo peak is seen only for B larger than the degeneracy field).

Our analysis of Fig. 3 leads us to conclude that the pronounced B-dependence of the tunnel conductance arises from a variety of Kondo regimes occurring for both odd and even occupation numbers. We should like to stress that the anomalous B -dependence does not seem to be a peculiarity of the device studied. Similar features have been observed also in other quantum dot devices as reported in Refs. 7,13, and 14. In some of these experiments, conductance modulations were surprisingly regular with a clear anti-correlation between adjacent Coulomb valleys (i.e., $G(B, V_g)$ looked like a chess board when plotted on grey scale). Evidently, all these observations cannot be explained in terms of the Anderson model and a pairwise filling of the dot levels. Instead the non-trivial multi-level structure of the dot and local electron-electron interactions are likely to play a key role, as already pointed out in Refs. 7 and 13.

It has been shown that in small quantum dots, such as the one considered here, electron-electron interactions can have important consequences on the ground state properties. For instance, Tarucha *et al.*¹² have identified B -driven spin transitions in a vertical quantum dot, discriminating between the contributions from local Coulomb and exchange interactions. In that experiment, as well as in Refs. 7,13,14 and in the experiment discussed here, the magnetic field was applied perpendicularly to the dot. In such a configuration, the field couples to the orbital motion of the confined electrons resulting in a strong influence on the electronic properties of the dot. (Note that a 0.1-T field is sufficient to have one quantum flux through the dot and break for instance time-reversal symmetry.)

We believe that ground-state transitions induced by the magnetic field are responsible for the onset of the Kondo-dominated regimes observed in Fig. 3. However, the nature of these transitions and their relation to the Kondo effect is unclear.

In the case of N =even, we know that ground-state transitions between singlet and triplet states produce an enhancement of the Kondo temperature. Therefore, B -driven transitions between $S=0$ and $S=1$ would lead to enhanced conductance near the points of spin degeneracy. In the case of N =odd, it is not known if spin transitions, for instance between $S=1/2$ and $S=3/2$, would also occur in a similar fashion. The mechanism responsible for the fluctuation of the Kondo temperature is quite obscure.

A more satisfactory physical picture can be formulated for the case of high magnetic fields. In the quantum Hall regime confined electrons occupy concentric shells associated with Landau levels. The outer shell has the best tunnel coupling to the leads and hence dominates the Kondo effect. Changing the field while keeping N constant causes electrons to move from one shell to another. Therefore the occupation of the outer shell can change without a variation in the total number of confined electrons (note that N can be either even or odd). By sweeping the field

the Kondo effect turns on and off depending on whether the occupation of the outer shell is odd or even, respectively. Starting from this simple picture, Tejedor and Martín-Moreno¹⁵ have recently proposed a more sophisticated model to explain the chess-board structure. Their analysis, however, applies only to the case of filling factors between 1 and 2. In our experiment this would correspond to $B > 2.5$ T, while conductance fluctuations are observed at much lower fields.

Finally, spin fluctuations could also be responsible for spin-blockade effects. Single-electron tunneling is suppressed whenever it involves two ground states differing in their spin by more than one unit. For instance, if two consecutive Coulomb valleys have $S = 0$ and $S = 3/2$ the conductance peak between them is suppressed. In Fig. 3A there are two narrow regions, one at $(B, V_{gl}) \approx (0.6 \text{ T}, -410 \text{ mV})$ and one at $(B, V_{gl}) \approx (1.1 \text{ T}, -420 \text{ mV})$, where the conductance peak may be suppressed due to spin blockade.

Acknowledgments

We acknowledge financial support from the Specially Promoted Research, Grant-in-Aid for Scientific Research, from the Ministry of Education, Science and Culture in Japan, from the Dutch Organisation for Fundamental Research on Matter (FOM), from the NEDO joint research program (NTDP-98), and from the EU via a TMR network.

References

1. A. C. Hewson, *The Kondo Problem to Heavy Fermions* (Cambridge University Press, Cambridge, 1993).
2. L. P. Kouwenhoven and L. I. Glazman, *Phys. World* **14**, 33 (2001).
3. L. I. Glazman and M. E. Raikh, *JETP Lett.* **47**, 452 (1988); T. K. Ng and P. A. Lee, *Phys. Rev. Lett.* **61**, 1768 (1988).
4. D. Goldhaber-Gordon *et al.*, *Nature* **391**, 156, (1998); Cronenwett *et al.*, *Science* **281**, 540 (1998); Schmid *et al.*, *Physica B* **256-258**, 182 (1998).
5. P. W. Anderson, *Phys. Rev.* **124**, 41 (1961).
6. S. Sasaki *et al.*, *Nature* **405**, 764 (2000).
7. J. Schmid *et al.*, *Phys. Rev. Lett.* **84**, 5824 (2000).
8. W. G. van der Wiel *et al.*, *Science* **289**, 2105 (2000).
9. D. Goldhaber-Gordon *et al.*, *Phys. Rev. Lett.* **81**, 5225 (1998); T. A. Costi *et al.*, *J. Phys. Condens. Matter* **6**, 2519 (1994).
10. W. Izumida, *et al.* *J. Phys. Soc. Jpn.* **70**, 1045 (2001).
11. M. Eto and Yu. Nazarov, *Phys. Rev. Lett.* **85**, 1306 (2000); M. Pustilnik *et al.*, *cond-mat/0010336*.
12. S. Tarucha *et al.*, *Phys. Rev. Lett.* **84**, 2485 (2000).
13. S. M. Maurer *et al.*, *Phys. Rev. Lett.* **83**, 1403 (1999).
14. M. Stopa, S. De Franceschi and L. P. Kouwenhoven, unpublished.
15. C. Tejedor and L. Martín-Moreno, *Phys. Rev. B* **63**, 035319 (2001).